PCCP

Accepted Manuscript

ROYAL SOCIETY OF CHEMISTRY

www.rsc.org/pccp

Physical Chemistry Chemical Physics
CREATED USING THE RSC LaTeX PCCP ARTICLE TEMPLATE – SEE www.rsc.org/electronicfiles FOR DETAILS
ARTICLE TYPE www. rsc.org/xxxxxx | XXXXXXXX

A Continuum Solvent Model of Ion–Ion Interactions in Water

Timothy T. Duignan,*[a] Drew F. Parsons,[a] and Barry W. Ninham[a]

Received Xth XXXXXXXXXX 20XX, Accepted Xth XXXXXXXXX 20XX
First published on the web Xth XXXXXXXXXX 200X
DOI: 10.1039/b000000x

The calculation of ion–ion interactions in water is a problem of long standing importance. Modelling these interactions is a prerequisite to explaining Hofmeister (specific ion) Effects. We here generalize our solvation model[1] of ions to calculate the free energy of two ions in water as a function of separation. The same procedure has previously been applied to calculate ion interactions with the air–water interface successfully.[2] The Conductor like Screening Model (COSMO) is used. This treats the ions on a quantum mechanical level and calculates numerically the electrostatic response of the surrounding solvent. Estimates of the change in the cavity formation energy and the change in the ion-water dispersion energy as the ions approach are included separately. The calculated interaction potentials are too attractive and this is a significant issue. However, they do reproduce the affinity of similarly sized ions for each other, which is a crucial property of these potentials. They are also oscillatory, another important property. We normalize the potentials to reduce the over–attraction, and good correlation with experimental values is achieved. We identify the driving contributions to this like–prefers–like behaviour. We then put forward a plausible hypothesis for the over–attraction of the potentials. An agreeable feature of our approach is that it does not rely on salt specific parameters deliberately adjusted to reproduce experimental values.

1 Introduction

Ion–ion interactions in water are central to understanding in a vast range of biological and industrial processes that involve electrolytes.[3,4] The most direct expression of ion–ion interactions in water are the osmotic and activity coefficients of electrolyte solutions. Activity/osmotic coefficients are a key to derived properties such as the pH, buffers osmotic pressure, chemical equilibria, specific heats, colloid interactions and many more. A parameter-free theory that predicts ion specific activities is therefore the goal. Specifically, what is required is a theory that minimises computation and is easily used by non–experts.

The activities are an important example of Hofmeister or Specific Ion Effects. Understanding and predicting these effects has long been a puzzle and a source of great frustration. These effects are observed universally in complex biological and chemical systems. But building an understanding of them must begin with the prototypical and simplest cases. We have already developed a model for two of these cases. The first is a continuum solvent model that predicts ionic solvation energies.[1] The second is a model of ionic interactions with the air–water interface.[2] These models were applied successfully to monoatomic and monovalent ions. Ion–ion interactions serve as a third example of these "simple" properties. The next challenge in building a consistent theory is therefore to tackle the problem of the interaction of a pair of ions in water. Were that goal to be accomplished we would have a firm foundation on which to attempt to build predictive quantitative models of more complex systems that show up in Hofmeister effects.

In a hierarchy of theoretical approaches we recall that the simplest so called "primitive" model of these properties is the Debye–Hückel theory.[5,6] It includes only the mean field ion–ion electrostatic interaction and a continuum solvent. A bulk liquid dielectric constant mediates (electrostatic) ion interactions. For real electrolytes, at very low concentrations the osmotic or activity coefficients depend only on the ionic valencies, and this model reproduces them well. At moderate concentrations, ion–specific short–range interactions become important. These were very difficult to model accurately, due to the changes in ion–water interaction with separation and direct non–electrostatic interactions of the ions. Further direct non–electrostatic interactions of the ions were ignored.

The next development from a practical viewpoint was to add extra (empirical) terms and parameters to the expressions derived from the Debye–Hückel model, in attempts to capture these short–range ion specific interactions. Two benchmark examples of this approach are those of Pitzer[7] and Bromley.[8] Bromley's formulation is particularly useful as it shows that the activity and osmotic coefficients of salts can be reproduced with reasonable accuracy up to moderate concentrations with only one parameter per salt. This parameter is analogous to a second virial coefficient, or B coefficient, in the case of a non–ideal gas. This dramatically simplifies the problem from a theoretical perspective, as the task is reduced to predicting only

[a] *Applied Mathematics Department, Australian National University, Canberra, ACT, 0200, Australia, Tel: +61 2 6125 2847; E-mail: tim.duignan@anu.edu.au*

these parameters, which have a clear physical interpretation, rather than having to reproduce the non–trivial concentration dependence of these properties. Important physically based extensions of the Debye–Hückel approach have also been developed,[9] as well as generalizations to asymmetric and mixed electrolytes.[10]

Numerous alternative approaches to modelling these properties have been considered. Some examples are HNC[11], NRTL,[12–14] MSA,[15–17] TPCP,[18,19] eCOSMO–SAC,[20] Monte Carlo or classical Molecular Dynamics (MD) simulation[21,22], hybrid implicit/explicit solvent approaches,[23,24] and *ab initio* MD approaches.[25–28] This incomplete list provides an indication of the variety of approaches taken to solve the problem.

An analysis of the comparative merits and limitations of these various approaches is outside our brief. However, we would point out that none of them have proven satisfactory. This is due to their complexity and a strong dependence on fitting parameters. These parameters are often adjusted for each salt. This limits their usefulness and obscures physical insight. The state of affairs is well captured by Kunz and Neueder in 2010, in the introductory chapter to Ref. 29, where they state: "there is not a single published work in which a prediction of these values can be found." Further "Today, it seems that the most physical model is one of the oldest: the Friedman–Gurney (FG) model" developed by Ramanathan and Friedman[11] in 1971. This model uses sophisticated HNC calculations to treat the statistical mechanics, but still relies on "Gurney potentials", with parameters adjusted for each salt. Improvements in the physical basis of models as well as their predictive and explanatory power are therefore crucially needed.

The bringing to bear of simulation to treat the position and orientation of water molecules explicitly does not appear to have moved us much closer to a predictive understanding of these interactions. Although these models can reproduce qualitative features of these interactions,[30] it appears that ion–ion interaction potential parameters and combining rules must be adjusted for each salt separately to reproduce these properties quantitatively.[31,32] In principle, this is not very different to relying on fitted Gurney potentials. It may be that only *ab initio* simulations,[27] will be capable of providing a model that does not rely on fitting. But their extreme computational demands make such a program very difficult to implement.

There is an alternative approach. This is to look for interesting correlations in the data, and interpret these using qualitative arguments or simplified models. Collins's[33] very useful "law of matching water affinity" exemplifies this approach. He argues that ions with similar water affinity, that is, similar ion-water interaction strength, are more strongly attracted to each other, and indeed this pattern is observed in osmotic or activity coefficients.[34,35] This can clearly be seen in Figure 1, where we plot the osmotic coefficients of several salts. As shown below, lower osmotic coefficients indicate a stronger solvent averaged ion-ion attraction. Intuitively, this is because stronger ion-ion attraction reduces the pressure the ions exert on the container walls. Figure 1 shows that ions with similar intrinsic size have lower osmotic coefficients. The intrinsic size of an ion also correlates roughly with its interaction strength with water. Hence, like–prefers–like is consistent with the "law of matching water affinity." This is a key observation on which it is necessary to remark further. Collins provides a qualitative argument to justify this law and Lund et al.[36] have provided a simple continuum solvent model of ion–ion interactions. This model qualitatively reproduces this like–like affinity of ions. The insights are real enough. But they fall short of the ultimate goal. This is to provide a model that can reproduce quantitatively the activity/osmotic coefficients of all salts without parameters fitted for each. Only then can we have confidence that the model has captured accurately the actual physical mechanisms that would allow a foundation for prediction and application to more complex systems.

The calculation of the direct ion–ion interactions in vacuum is a relatively straightforward task using modern quantum chemistry software. The fundamental difficulty in predicting these interactions in water is ionic hydration, i.e., the interaction of the ions with the water molecules around them and how this interaction changes as the two ions come together. The basic problem therefore amounts to calculating how the solvation energy of the two ions changes as they come together. We have developed a satisfactory model of solvation energies.[1,37,38] We can therefore generalize this solvation model to the case of two ions in close proximity to each other. A knowledge of this solvation model will therefore be very useful in understanding the method applied here.

We have recently used this approach to calculate ion interactions with the air–water interface.[2] The results are encouraging and invite extension to other properties of electrolyte solution. If that works, the assumptions of the model are reinforced. This will also reduce the need for more fitting parameters, our main aim. Ref. 39 used this approach. A model for osmotic coefficients was fitted to determine the dispersion interaction contributions by adjusting the polarizabilities and ionic sizes. These ion–specific interactions are missing from conventional approaches. It was then generalized to determine ion–surface interactions. Although the model had limited success due to some neglected contributions, the general approach is still suggestive.

2 Theory

The solvent averaged free energy of interaction of two ions is taken to be given by the expression

$$G(d) = G_{\mathrm{COSMO}}(d) + \Delta G_{\mathrm{cav}}(d) + \Delta G_{\mathrm{disp}}(d) \qquad (1)$$

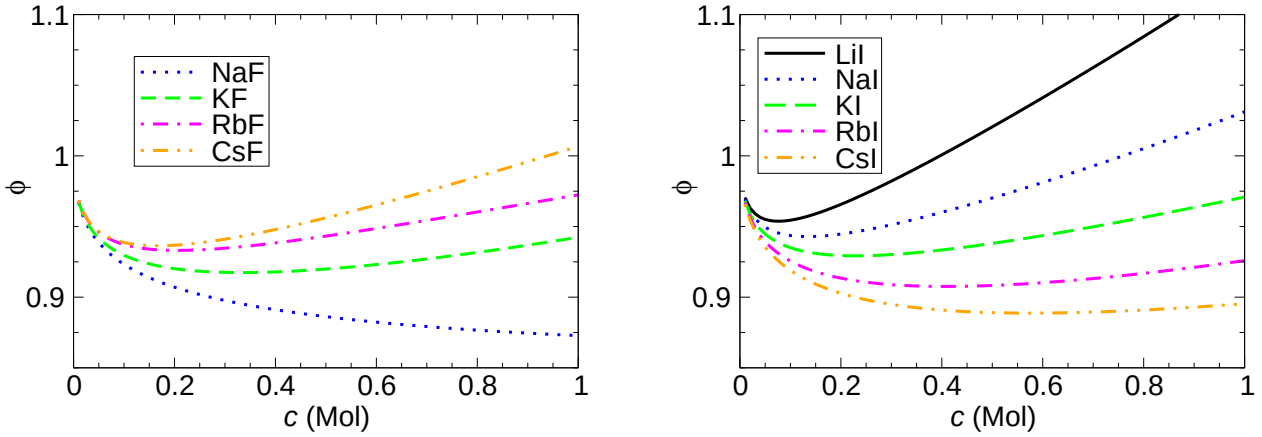

(a) Fluoride salts

(b) Iodide salts

Fig. 1 The osmotic coefficients of the fluoride and iodide salts exhibit the like prefers like behaviour. Ions of similar size have the lowest osmotic coefficient and hence the strongest attraction.

Each of these three terms is a generalization of one of the three terms in our solvation model.[1] $G_{\mathrm{COSMO}}(d)$ corresponds to the change in the electrostatic Born solvation energy plus the direct ion–ion interaction. $\Delta G_{\mathrm{cav}}(d)$ and $\Delta G_{\mathrm{disp}}(d)$ give the change in the cavity formation energy and the ion–water dispersion interaction energy of the two ions as the approach each other. Each of these terms is described in more detail in the following sections. The cavity and van der Waals (dispersion) interactions are missing from standard treatments in which the first term would be an electrostatic interaction with, e.g., a hard core cut–off.

This interaction energy will be used to determine experimental activity and osmotic coefficients. We discuss this in the Experimental Values section below.

2.1 Direct Electrostatic Contributions

As two ions come together they experience a direct electrostatic interaction. At large separations (several water molecules) this is given to a good approximation by Coulomb's law with the static dielectric constant of water used.

$$G_{\mathrm{Coulomb}} = \frac{e^2}{4\pi\varepsilon_o\varepsilon_w r} \tag{2}$$

The dielectric constant of water has its bulk static value. At large separations and at infinite dilution the Coulomb term is the only contribution to the interaction. It is used in the derivation of the original Debye–Hückel model, which is the origin of the non–ion specific term in the Pitzer and Bromley equations.

However, at short–range this expression is inaccurate. This is because it assumes that the ions are point charges imbedded in the dielectric medium. It is often asserted that at small separations, i.e., where r is of the order of the size of a molecule, the continuum solvent approximation will break down and explicit solvent or more sophisticated treatments will be necessary. Although on the face of it this seems like a reasonable statement it is worth testing, by building the best possible continuum models we can, and looking at their degree of accuracy. There are several potential improvements of the simple continuum solvent model that can still be made. In the context of the electrostatic interaction this means including the change in geometry,[40] magnitude[21] or isotropy[41] of the dielectric as the two ions come together.

More specifically, as the two ions approach there will eventually come a point where the separation is so small that a water molecule can no longer fit between them. There will be some substantial cost to removing this water from the surfaces of the ions. But there will be a corresponding increase in attraction of oppositely charged ions, due to the decrease in the effective dielectric constant of the medium between them. These effects arise because the ions occupy finite sized cavities in the water where the relative dielectric constant is 1. To take care of this problem we need the solution of Poisson's equation with the complex boundary condition created by the two overlapping spherical cavities.

We can use a numerical approach to model this situation approximately with the Conductor Like Screening Model COSMO).[42,43] This model treats the solutes on a quantum mechanical basis. The water is approximated as a conductor, and

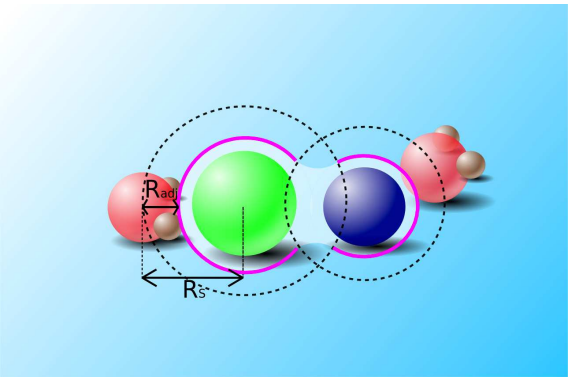

Fig. 2 Depiction of the COSMO calculation of the ion–ion interaction. The pink line shows the surface of the cavity where the surface charges are located.

the interface between the cavity occupied by the solutes and the background medium is determined from the Solvent Accessible Surface Area (SASA). The electric field of the solutes induces a surface charge on this interface. The calculation proceeds until self–consistency is reached. This calculation is depicted in Figure 2. The advantages of this approach are: Firstly, it includes the repulsion due to the loss of electrostatic ion–water interactions upon the removal of water from the first hydration layer. Secondly, it includes the reduced damping of direct ion–ion interaction, due to the removal of water. Thirdly, it provides an accurate calculation of the direct ion–ion interaction as both solutes are treated at a quantum mechanical level. This quantum mechanical treatment does mean that the COSMO calculation includes the direct ion–ion dispersion interaction and Pauli repulsion of the two ions. Hence, it is not purely an electrostatic calculation.

This calculation can be thought of as the direct ion–ion interaction plus the change in Born energy of the two ions as they come together. This is consistent with the fact that the COSMO calculation of the two ions at infinite separation gives the Born solvation energy of the two ions. The calculation details are provided below. If the cavities do not overlap, the COSMO calculation reproduces the normal Coulomb interaction. The methodology is in principle the same as the one presented by Rashin[40] and Pratt *et al.*,[44] except that we have applied a more sophisticated quantum treatment of the ion.

2.2 Cavity Energy

The next contribution to the ion–ion interaction is that as they come together the water removed will move back into bulk. There will be some energy gain associated with this due to the fact that there is an energy of forming the cavity in water that the ion occupies, which is now released. This has been put forward by Collins[33] as a key mechanism driving the experimentally observed affinity of large ions for each other. It has also been identified as a key driver of anionic adsorption to the air water interface.[2,45] This can be thought of as a hydrophobic attraction, although it may not have the usual entropic character.[38]

In our solvation model[1] the energy of forming a cavity is calculated by multiplying the surface area of the cavity by the surface tension of the bulk air–water interface. This is different to the cavity formation energy of small neutral solutes, which is smaller and entropically dominated. The reason for this difference is that water molecules can form a hydrogen bonded network around a neutral molecule.[46] This is not applicable to ions, which will reorient nearby water molecules and break this structure.

The use of bulk interfacial tension can obviously be disputed. However we have used it in other applications[1,2,38] where it works reasonably well.

We therefore use the same bulk interface surface tension to calculate the cavity contribution to the ion–ion interaction energy. For instance for solutes i and j in contact, we have:

$$\Delta G_{\mathrm{cav}} = \sigma_{\mathrm{ion}}\left(\Delta A_i(d) + \Delta A_j(d)\right) \tag{3}$$

where $\sigma_{\mathrm{ion}} = 0.434\ \mathrm{kJmol^{-1}\AA^{-2}}$. $\Delta A_i(d)$ is the change in surface area of ion i due to the presence of ion j as a function of separation, and vice versa for $\Delta A_j(d)$. The change in area is straightforwardly determined by the area of the spherical cap that is removed when the two ions overlap.[47]

$$\Delta A_i(d) = \begin{cases} -\pi R_{\mathrm{S},i}\left(R_{\mathrm{S},i} + R_{\mathrm{S},j} - d\right)\left(1 + \frac{R_{\mathrm{S},j} - R_{\mathrm{S},i}}{d}\right) & d < R_{\mathrm{S},i} + R_{\mathrm{S},j} \\ 0 & d \geq R_{\mathrm{S},i} + R_{\mathrm{S},j} \end{cases} \tag{4}$$

$R_{\mathrm{S},i}$ is the R_{S} parameter of ion i, defined as the distance to the peak in the solute–oxygen radial distribution function.[37] Similarly, we have:

$$\Delta A_j(d) = \begin{cases} -\pi R_{\mathrm{S},j}\left(R_{\mathrm{S},j} + R_{\mathrm{S},i} - d\right)\left(1 + \frac{R_{\mathrm{S},i} - R_{\mathrm{S},j}}{d}\right) & d < R_{\mathrm{S},j} + R_{\mathrm{S},i} \\ 0 & d \geq R_{\mathrm{S},j} + R_{\mathrm{S},i} \end{cases} \tag{5}$$

2.3 Dispersion

2.3.1 Ion–Water Dispersion. The next important contribution is the change in the ion–water dispersion interaction. The simplest approximation to this energy is to assume that it decreases in proportion to the change in the surface area. This is the approximation we have used in the case of the ion interaction with the air–water interface. However, this will not work in this situation as the water molecules are not being removed completely from the ion as they are in the case of an ion at the air–water interface, but simply displaced to a distance slightly further away. The accurate computation

of this energy would require the calculation of the Green's function with the boundary condition given by the overlapping cavity. This is equivalent to solving Poisson's equation for these rather complicated geometrical configurations. This task is underway, but significant difficulties remain. We can use an approximation in between these two approaches. We assume that the dispersion solvation energy is approximately pairwise additive, with a C_{2n}/r^{2n} behaviour. $n = 3$ for the dipolar dispersion energy $n = 4$ for the quadrupole term and $n = 5$ for the octupole term. In other words, we assume:

$$G_{\mathrm{D}} = \int d^3\mathbf{r}'\rho(\mathbf{r}')\frac{C_6}{|\mathbf{r}'-\mathbf{r}_i|^6} \tag{6}$$

$$G_{\mathrm{Q}} = \int d^3\mathbf{r}'\rho(\mathbf{r}')\frac{C_8}{|\mathbf{r}'-\mathbf{r}_i|^8} \tag{7}$$

$$G_{\mathrm{O}} = \int d^3\mathbf{r}'\rho(\mathbf{r}')\frac{C_{10}}{|\mathbf{r}'-\mathbf{r}_i|^{10}} \tag{8}$$

Where the G_{D}, G_{Q} and G_{O} are the same as defined in Ref. 37. For $\rho(\mathbf{r}')$ we use a function that is ρ_w outside the cavity and 0 inside it. This function is therefore dependent on the distance between the two ions, as well as the size of the cavities etc. We therefore write it as $\rho(\mathbf{r}',d)$.

We can then write the change in dispersion interaction as a function of separation:

$$\Delta G_{\mathrm{D}}(d) = \left(\frac{\int d^3\mathbf{r}'\rho(\mathbf{r}',d)\frac{C_6}{|\mathbf{r}'-\mathbf{r}_i|^6}}{\int d^3\mathbf{r}'\rho(\mathbf{r}',\infty)\frac{C_6}{|\mathbf{r}'-\mathbf{r}_i|^6}} - 1\right)G_{\mathrm{D}} \tag{9}$$

$$\Delta G_{\mathrm{Q}}(d) = \left(\frac{\int d^3\mathbf{r}'\rho(\mathbf{r}',d)\frac{C_8}{|\mathbf{r}'-\mathbf{r}_i|^8}}{\int d^3\mathbf{r}'\rho(\mathbf{r}',\infty)\frac{C_8}{|\mathbf{r}'-\mathbf{r}_i|^8}} - 1\right)G_{\mathrm{Q}} \tag{10}$$

$$\Delta G_{\mathrm{O}}(d) = \left(\frac{\int d^3\mathbf{r}'\rho(\mathbf{r}',d)\frac{C_{10}}{|\mathbf{r}'-\mathbf{r}_i|^{10}}}{\int d^3\mathbf{r}'\rho(\mathbf{r}',\infty)\frac{C_{10}}{|\mathbf{r}'-\mathbf{r}_i|^{10}}} - 1\right)G_{\mathrm{O}} \tag{11}$$

The density of water and the dispersion constants cancel out, and these expressions can be calculated analytically using toroidal coordinates. This calculation is presented in the appendix.

This allows a calculation of the change in ion–water dispersion interaction at contact. We then assume that this interaction scales with the change in surface area of the ions. This is for several reasons: Firstly, for ease of computation, which would otherwise require the use of bispherical coordinates at larger separations. Secondly, because the cavity formation and dispersion energy should have similar distance dependence as both arise from the removal of water. Thirdly, for consistency with our previously developed model of ion–surface interactions where this approximation worked well. The expression is therefore given by:

$$\begin{aligned}\Delta G_{\mathrm{disp}}(d) = &\left(\Delta G_{\mathrm{D},i}(d_{\mathrm{c}}) + \Delta G_{\mathrm{Q},i}(d_{\mathrm{c}}) + \Delta G_{\mathrm{O},i}(d_{\mathrm{c}})\right)\frac{\Delta A_i(d)}{\Delta A_i(d_{\mathrm{c}})} \\ &+\left(\Delta G_{\mathrm{D},j}(d_{\mathrm{c}}) + \Delta G_{\mathrm{Q},j}(d_{\mathrm{c}}) + \Delta G_{\mathrm{O},j}(d_{\mathrm{c}})\right)\frac{\Delta A_j(d)}{\Delta A_j(d_{\mathrm{c}})}\end{aligned} \tag{12}$$

Where d_{c} gives the separation of the ions in contact. For this we use the sum of the crystal radii of the ions, given in Ref. 37. This is approximately the position of the minimum in the ion–ion interaction potential.

2.3.2 Ion–Ion Dispersion. We have previously suggested[35] that the direct ion–ion dispersion interaction plays a significant role in the affinity of large ions for each other in water. This contribution can be included in the COSMO calculation by using an MP2 level of theory. Hence, it does not need to be calculated separately, i.e., the term $G_{\mathrm{COSMO}}(d)$ includes both the electrostatic and ion–ion dispersion interactions. We can probe the importance of this interaction by comparing calculations at the MP2 level and the Hartree–Fock level. The difference is likely to be predominantly due to the dispersion interaction, as the dispersion interaction arises entirely from the intermolecular correlation effects included in the MP2 level but not at the Hatree–Fock level. This is clear from the interaction of noble gas atoms where the difference between these two levels of theories is very close to analytical calculations of the dispersion interaction. This calculation does neglect the many body correction to this interaction due to the presence of the surrounding water molecules, that may be on the order of 10%.[48] Including this contribution would again require the Green's function with the given boundary conditions.

2.4 Experimental Values

The most rigorous approach to compare our interaction potentials with experiment would be to use the solvent averaged ion–ion interactions to calculate the activity/osmotic coefficients accurately at all concentrations using relatively sophisticated statistical mechanics, such as HNC calculations[11] or simulations.[23] These calculations are prone to numerical difficulties, and are sensitive to small perturbations in the interaction potential.[22] We adopt a simpler approach.

We start with the osmotic and activity coefficients of a solute that only interacts only via short–range interactions with other solutes at low concentrations. The osmotic coefficient is given by:[49,50]

$$\phi(c) = 1 + Bc \tag{13}$$

and the activity coefficients by:

$$\ln\gamma(c) = 2Bc \tag{14}$$

where B is the second virial coefficient:

$$B = -2\pi \int_0^\infty dr r^2 \left(e^{-\beta G(r)} - 1 \right) \quad (15)$$

Here $G(r)$ is the free energy of interaction of two solutes as a function of separation. We use the variable r instead of d for clarity. The situation is significantly more complicated for ions because they undergo long–range electrostatic interactions, and so these expressions are invalid. However, this long–range electrostatic interaction depends only on the valency of the ions. It is well established that ion–specificity, for ions of the same valence, is primarily attributable to the short–range interactions. If we assume that these two effects make additive contributions, then we can write the osmotic coefficients as:

$$\phi_{ij}(c) = 1 + f_\phi(c) + B_{ij}c \quad (16)$$

and the activity coefficient as

$$\ln \gamma_{ij}(c) = f_\gamma(c) + 2B_{ij}c \quad (17)$$

Where $f_\phi(c)$ and $f_\gamma(c)$ depend only on the valency of the ions and are attributable to the long–range electrostatic Coulomb interaction, while the ion–specificity is captured by the B_{ij} parameter.

Indeed, this expected behaviour is approximately correct. The Specific Interaction Theory (SIT)[51] shows that these values can be reasonably well captured over a range of concentrations using only one parameter (B_{ij}) per salt. In SIT the Debye–Hückel expression is used to calculate the Coulomb term's contribution:

$$f_\gamma(c) = \frac{A\sqrt{c}}{1 + 1.5\sqrt{c}} \quad (18)$$

This simple formulation of the ion–specific variation is consistent with Figure 1, where the osmotic coefficients do not cross, but simply spread out as concentration increases. More exactly, the difference between the osmotic coefficients of two different salts as a function of concentration is approximately a straight line though the origin, which supports this formulation.[52] The activity coefficients behave similarly.

This provides a much simpler and more direct means of testing theoretically calculated potentials, and bypasses the need to perform complex concentration dependent calculations. We can take our solvent averaged ion–ion potentials, subtract the long–range Coulomb interaction and then substitute this potential into Eq. 15. In principle, the resulting values should approximately agree with the B_{ij} parameters derived from experiment. Although this procedure is approximate the error is likely to be less than that associated with a continuum solvent approximation and more sophisticated calculations should be possible once a satisfactory model is discovered. Reproducing the B_{ij} parameters is practically equivalent to reproducing the osmotic and activity coefficients over a large concentration range and with reasonable accuracy. The simplest model[9] for the B_{ij} parameter is to assume a hard sphere potential, in which case Eq. 15 reduces to: $\frac{2}{3}\pi a^3$, where a is the size of the ions. However, this model is unsatisfactory as the ion sizes must be adjusted to unphysical values, and are not additive, that is, the size depends on the counterion.

SIT is very similar to the Pitzer and Bromley formulations with some exceptions. Firstly, some empirical adjustments are made to the parameters of the $f(c)$ term to improve agreement. Secondly, in Bromley's model the B_{ij} parameter has a weak concentration dependence. Thirdly, in the Pitzer formulation there are some additional higher order salt specific parameters. These differences are not too important and only improve agreement by a few per cent, or extend the concentration range. Hence, for our purposes the three approaches are equivalent and we can compare with the B_{ij} parameters from any approach and reach similar conclusions.

We will compare our calculations with the parameters determined by Bromley. This is because this is a single parameter formulation, which achieves agreement over a wide concentration range, and the values have been tabulated for a large number of ions. The conclusions are very similar if we compare with the $\beta^{(0)}$ parameters of Pitzer's model,[7] or the ε_0 parameters of SIT.[51] In addition, technically we should compare with B_{ij} coefficients adjusted to reproduce the activity coefficients after adjustment to the McMillan–Mayer[53] system as well as adjustment to molarity for the concentration units. This more rigorous approach has been completed and does not alter the conclusions of the work significantly; we therefore neglect it for simplicity.

Evidence indicates that the cation–cation and anion–anion short–range interactions are not too important at low to moderate concentrations as Coulomb repulsion prevents them from approaching close enough to each other. Hence, we assume that it is a reasonable approximation in calculating the B_{ij} parameter to use only the cation–anion interactions.[22]

2.4.1 Collins's Rules. We will refer to the B coefficients determined by Bromley as B_{Brom}. These B_{Brom} parameters show an intriguing regularity when plotted as a function of difference in the solvation energy of the ions.[35] This can be seen below in Figure 4a, where they are compared with the theoretically calculated values. Although the trend appears inverted, the values are consistent with the classic "Volcano behaviour."[33] Hence, they reflect Collins's "Law of Matching Water Affinity." Ions with similar solvation energies have the lowest B_{Brom} coefficients and hence have the lowest osmotic and activity coefficients and are most strongly attracted to each other. Reproducing these B_{Brom} coefficients should therefore

also mean this useful and puzzling correlation has been explained.

3 Calculation Details

The calculation details are very similar to those used in Ref. 2. We used the TURBOMOLE package (v6.4)[54,55] with COSMO[42,43] implemented. The def2–QZVPP[56–59] basis sets, and associated ECPs[60,61] were used for all nine alkali and halide ions. We did not use def2-QZVPPD due to implementation constraints of RIMP2, and because there is some evidence diffuse basis sets do not work well with a continuum solvent model.[62]

The calculations were performed both at the Hartree–Fock level using the DSCF program[63] and at the MP2 level using the RIMP2 program.[64–66] There is some evidence that the MP2 level of theory may overestimate dispersion interactions somewhat, compared with the more accurate CCSD(T) level.[67] For a more quantitatively exact approach it would be preferable to use this higher level. There are implementation problems with this approach however and the error is likely substantially less than that associated with the continuum approximation.

For the cavity sizes in the COSMO calculation we use the cavity sizes determined in the original solvation model. They are referred to as R_{cav} and shown in Table 1. They are given by $R_{\mathrm{cav}} = R_{\mathrm{S}} - R_{\mathrm{adj}}$, where $R_{\mathrm{adj}} = 0.84$ Å. This was justified in Ref. 37, where they were originally determined. Using these cavity sizes leads to an error in the solvation energies of 12 kJ mol^{-1} (3%). This error will result in some corresponding error in the ion–ion interactions, as a result of the fact that the total solvation energy is not correctly modelled. In order to reduce this error, we adjust R_{cav} to the nearest 0.01 Å to minimize the error in the solvation energies. It is reasonable to adjust these values, as they are the largest source of error in the model. This is due to the fact that the solvation energies are quite sensitive to these values and they are difficult to determine accurately. This adjustment reduces the mean unsigned error in the solvation model to 1 kJ mol^{-1}, which should allow for improved agreement with ion–water interaction potentials. These values are referred to as R_{cavA} and are given in Table 1. The R_{S} values are also altered to satisfy the relationship $R_{\mathrm{S}} = R_{\mathrm{cav}} + R_{\mathrm{adj}}$.

COSMO's RSOLV parameter was set to 0.84 Å. This is because it is equivalent to the R_{adj} parameter we have used here. They both give the distance from the surface of the cavity to the centre of the solvent molecule. An open cavity was constructed for simplicity and consistency with Ref. 2. The outlying charge correction was included although the ROUTF parameter had to be reduced to 0.3, due to numerical error with the default value. The epsilon parameter was set to 116.95 to reproduce the correct 1/78.3 damping of the Coulomb interaction. The ion–specific short–range interaction has a negligible dependence on this parameter.

Table 1 Values of the cavity sizes of the ions in water. R_{cav} is taken from Ref. 37. R_{cavA} is determined by adjustment that minimize the deviation from experimental bulk solvation energies. This table is reproduced from Ref. 2

Ion	R_{cav}(Å)	R_{cavA}(Å)
Li^+	1.22	1.24
Na^+	1.51	1.55
K^+	1.95	1.94
Rb^+	2.08	2.11
Cs^+	2.27	2.31
F^-	1.84	1.84
Cl^-	2.36	2.41
Br^-	2.51	2.59
I^-	2.80	2.83

Both sets of radii have been used in order to compare with experiment. An identical procedure was carried out for the ion–water interactions in Ref. 2 where it improved experimental agreement slightly, as expected.

4 Results and Discussion

4.1 Interactions

The interaction potentials calculated using the above method are shown in Figure 3. The most obvious and concerning observation is that the attraction between two ions is too large to be physical. The potential wells should be of the order of a few $k_{\mathrm{B}}T$. Here they can exceed $-20k_{\mathrm{B}}T$.

Nonetheless there are two encouraging features of these potentials. Firstly, and most clearly evident for small ions, there is an oscillatory character to the interaction potentials. This character is consistent with simulation and is occasionally used as justification for the necessity of explicit solvent approaches. This calculation shows that it is possible to predict an oscillatory potential solely on the basis of a continuum approach. This was originally pointed out by Rashin.[40] Indeed, if the Hartree-Fock level of theory is used with the same cavity sizes chosen by Rashin in the COSMO calculation, the calculated potentials are consistent with the ones in Ref. 40. The contributions to these potentials are discussed below, and Figure 6 shows that it is the COSMO contribution that drives this oscillation. It arises from the lost ion–water electrostatic interaction as the solvent is removed from the surface of the ion. This results in a repulsion when the ionic cavities first overlap. This repulsion is then overcome by the large electrostatic attraction, which is no longer damped by intervening solvent molecules. However, the oscillatory character is

not observed for the larger ions. This is presumably another symptom of whatever is causing the large over–attraction in the potentials. Indeed, by reducing the cavity size arbitrarily we can prevent the over–attraction and a qualitatively correct oscillatory interaction emerges. We should point out that the attractive surface area term, which is analogous to a hydrophobic attraction, should have an oscillatory character as well. It arises from the changing environment from one containing bulk water molecules to a vacuum as the two ions come together. It is clear from simulation of neutral molecule interactions in water, and could be partially included in the model with a more sophisticated definition of the change in surface area.[68] Also only one peak in the oscillation is present as the removal of discrete second and third water layers is not modelled.

The second promising feature of these potentials is that they appear to be consistent with Collins's "law of matching water affinity", i.e., like–prefers–like. For instance, Figure 3a shows the interactions of the lithium ion. We see that as the anion increases in size the interaction becomes more repulsive. Whereas for cesium's interactions (Figure 3b), as the anion increases in size, the potential well widens but the depth remains relatively constant. This will be countered to some extent by the additional repulsion from the larger ion sizes.

This Hofmeister series reversal with activities has been noted previously,[34] and is clear from Figure 4a. This reversal is also apparent between iodide and fluoride salts. This is consistent with Collins's law, and Figure 6 below provides physical insight into its cause.

4.2 Experimental Comparison

It is useful to have a quantitative comparison of the theoretical ion–ion affinity with experiment. It is clear that we cannot use these potentials to directly to calculate B coefficients. (Eq. 15) The exponential term combined with potentials that are much larger than thermal energy means there will be huge variation in these calculated B values, in clear disagreement with experiment. The simplest and most straightforward fix to this problem is to normalize the potentials to reduce them to a size on the order of thermal energy. If we divide all of the potentials by a factor (λ) and then calculate the B coefficients, we achieve much better results. That is:

$$B_{\text{Theory}} = -2\pi k \int_0^\infty dr r^2 \left(\exp^{-\beta G(r)/\lambda} - 1\right) \qquad (19)$$

where

$$G(r) = \left(G_{\text{COSMO}}(r) + \frac{e^2}{4\pi\varepsilon_w r} + \Delta G_{\text{cav}}(r) + \Delta G_{\text{disp}}(r)\right) \qquad (20)$$

and where $k = 2/\ln(10)$ is a conversion factor which allows B_{Theory} to be compared directly with B_{Brom}. If Ångstroms are used in the calculation then an additional factor of $N_A\rho_w \times 10^{-30}$ is needed to convert to kg mol^{-1}. The theoretical values calculated with Eq. 19 have a good linear correlation with the experimental Bromley B coefficients. If $\lambda = 6.9$ then $R^2 = 0.95$. This value is insensitive to the choice of lambda, with the correlation staying above $R^2 = 0.9$ for $\lambda = 4.3 \rightarrow 22$. This level of agreement cannot be explained by chance and the physics must be correctly captured to some degree. With $\lambda = 6.9$ the resulting linear correlation has a slope of 1. The resulting B coefficients thus calculated are shown in Figure 4b. It is immediately clear that the behaviours seen in Figure 4a are reproduced, although with some error. The largest affinity of sodium fluoride and cesium iodide is reproduced. The upturn for the fluoride salts is also reproduced, as is the linear trend for the smaller alkali cations. Figure 5 shows the more direct comparison. With the unadjusted cavity radii the correlation is significantly worse ($R^2 = 0.84$).

As the correlation has a slope of 1 only a constant needs to be added to the theoretical values in order to predict the experimental values. This constant is 0.13 if R_{cavA} are used. It is essentially an additional fitted parameter. It is non–ion specific and accounts for the deviation of Bromley's B coefficient from the ones defined here. There could be several causes of this deviation. One could be that there is a contribution from the like charge interaction, which we neglect. Alternatively, it could arise from the fairly artificial process of applying the damping parameter λ. It could also be an issue arising from the splitting of the Coulomb and short–range interaction into additive contributions. Calculating the real potentials from those calculated here is likely a more complex task. The key point is that this parameter is not salt specific and so the model should be able to provide improved predictability and explanatory power, over existing models that often depend on salt specific parameters.

Reproducing the ion–specific trends in the activity coefficients has been a long–standing and central goal of physical chemistry for nearly a century. During this time there has been limited success in reproducing these trends without the use of parameters fitted to each salt. Here we reproduce the trend with good accuracy for all nineteen soluble alkali halide salts. Two parameters reproducing 19 values with such a good correlation is strong evidence that the Hofmeister trends have been correctly modelled. We emphasize that apart from the damping parameter and the offset constant, there has been no deliberate adjustment of parameters to reproduce desired properties of the interaction potentials. They are determined from a straightforward generalization of our solvation model.

4.3 Possible Causes of Over–Attraction

Although the good correlation seen in the theoretical comparison (Figure 5) is compelling, we need to answer the ques-

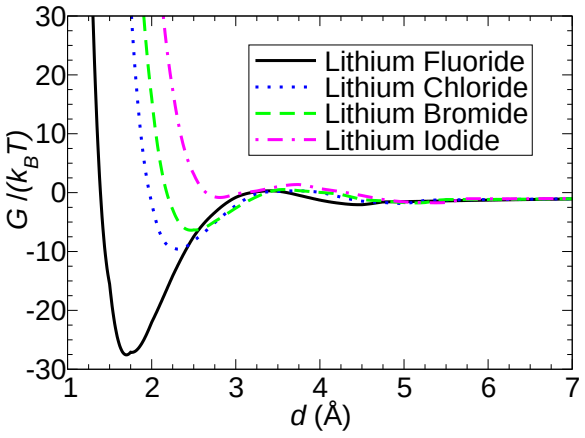

(a) Lithium salts

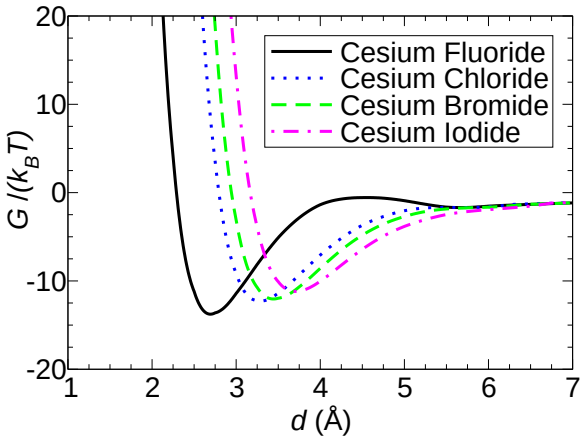

(b) Cesium salts

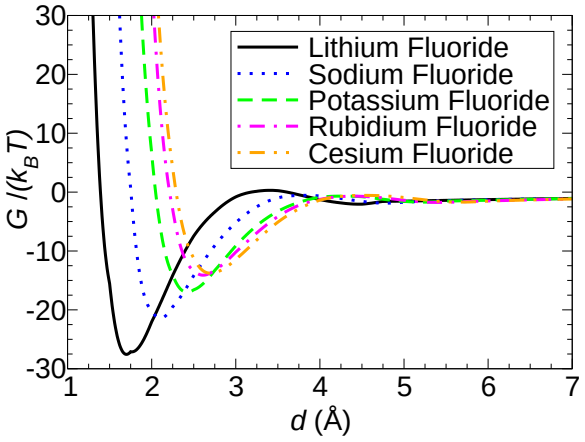

(c) Fluoride salts

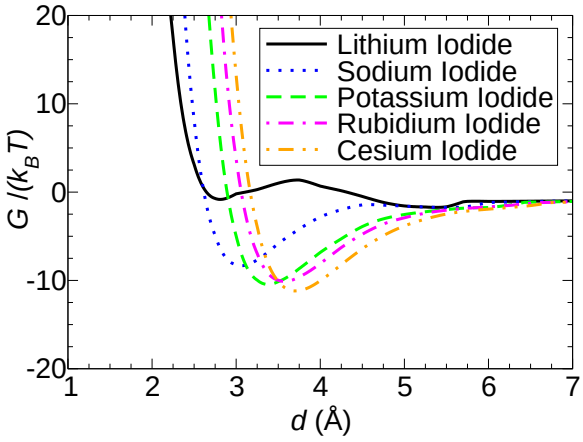

(d) Iodide salts

Fig. 3 Ion–ion interaction potentials. Calculated using R_{cavA}.

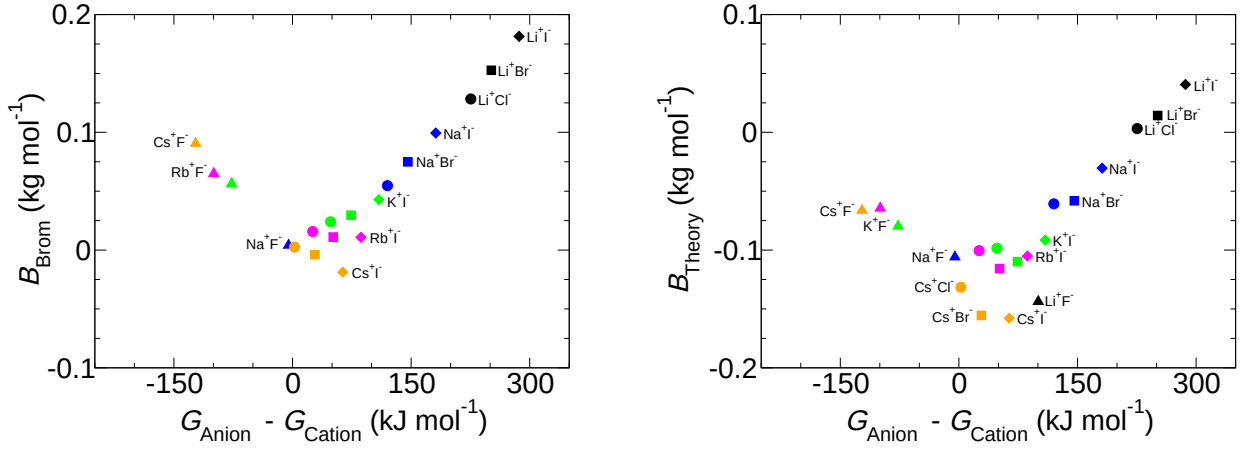

(a) Experimental Bromley B coefficients **(b)** Theoretical B coefficient.

Fig. 4 Theoretical and experimental B coefficients vs. the difference in the solvation energy of the ions. Colours indicate the cation: Lithium: Black, Sodium: blue, Potassium: green, Rubidium: magenta and Cesium: orange. Anions are marked with a symbol: Fluoride: ▲, Chloride: ●, Bromide: ■, Iodide: ◆. R_{cavA} is used, this is the cavity size adjusted to best reproduce bulk solvation energies.

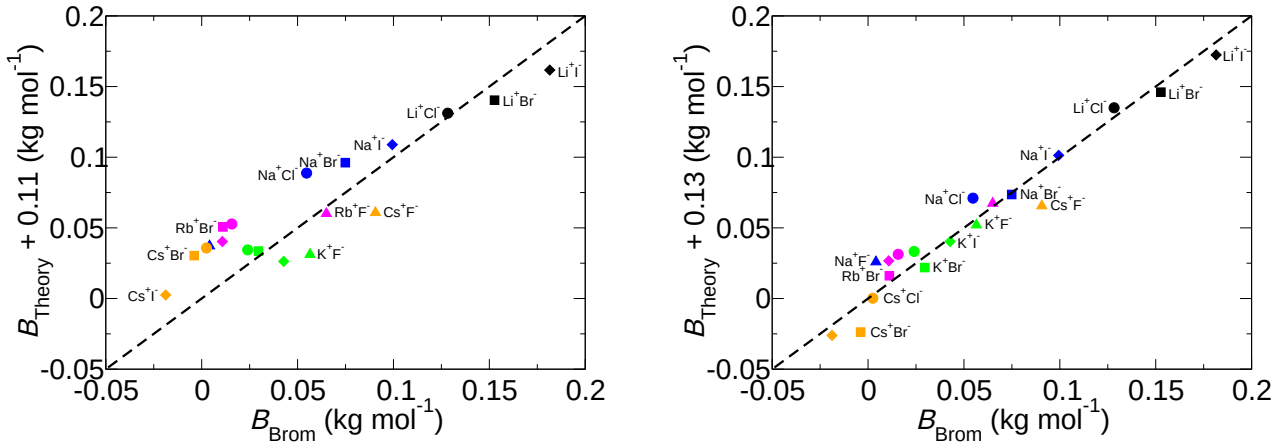

(a) With R_{cav} **(b)** With R_{cavA}

Fig. 5 Comparison of the theoretical B coefficients with Bromley's values.

tion of how the potentials could be so strongly over–attractive. This over–attraction of ion pairs has been observed previously.[44,69] To a lesser degree, it also occurs in continuum solvent models applied to more complex protein systems,[70,71] as well as in non–polarizable explicit solvent simulations of ion–pairing.[30,72] These studies put forward various physical explanations of this effect and introduce empirical corrections to account for it.

One straightforward explanation is that there is some missing repulsive contribution. For instance, as the two ions come together their electric fields will partially cancel. This may result in a reduced attraction with the surrounding water molecules, which then relax away from the ions. This would effectively cause an increase in the R_{cav} parameters. The corresponding energetic cost could substantially cancel the large attractive potentials calculated here.[73] Alternatively, entropic effects associated with the discrete water molecules may be important. It is plausible that the simple continuum solvent approach cannot account for these effects. For instance, an ordered profile of water molecules will form around an ion. This may lead to an entropic repulsion as that profile is disturbed. This is in essence the mechanism identified in Ref. 74. Similarly, it appears that there is a substantially enhanced solvent ordering around ion pairs.[30] Again this would provide an entropic repulsion which may be neglected by the continuum approach. Additional possibilities are a loss of electronic ion–water interactions,[27] bridging water molecule effects,[75] or inadequate dielectric screening at short–range. These explanations apply only to ion-pairs. This is important because the same approach appears to work well without any damping when applied to ion-surface interactions and to single ion solvation energies.

However, an issue with these explanations is that if there is some missing repulsive contribution of the size of $\approx 10k_{\mathrm{B}}T$, presumably it would play an important role in determining the ion–specificity. How can the correct Hofmeister trends be reproduced with such a large missing contribution? One plausible answer lies in the notion of entropy–enthalpy compensation. It is known that ion–ion interactions are the result of the cancelling of an entropic attraction and enthalpic repulsion.[76] It is possible that the entropic component has been overestimated, and hence the potentials are too attractive. This is consistent with the fact that the underlying solvation model calculates entropies of solvation that are too negative if not corrected to account for dielectric saturation effects.[38] This amplification of the entropy changes may lead to the over attraction. The dampening of these potentials to bring them into line with the expected size, can therefore simply be interpreted as a means of artificially imposing entropy–enthalpy cancellation, and hence is all that is required to achieve quantitative agreement with experiment.

4.4 Mechanism of Collins's law

Having established a plausible candidate for the cause of the over–attraction. We can investigate the contributions to the ion–ion interactions in order to determine a physical explanation of the like–prefers–like behaviour. We assume that the relative balance of contributions will be the same in the true interaction as they are in the overly attractive ones calculated here. If this were not the case, it is difficult to see how the correct Hofmeister trends could be so well reproduced. These contributions are shown in Figure 6, where the interactions of representative large–large, small–small, small–large and large–small pairs are presented. We omit lithium fluoride, as it is insoluble.

4.4.1 COSMO Contribution. The G_{COSMO} term includes contributions from the ion–ion dispersion interaction and Pauli repulsion as well as the ionic electrostatic interaction. We can identify several important behaviours of this contribution. For small pairs, there is a substantial cost to removing the tightly bound water resulting in a repulsion at larger separations. A large attraction, likely from direct electrostatics, cancels this effect at short–range, and results in a narrow and deep potential well at contact. As one of the ions gets larger, two effects come into play; the water is less tightly bound to the large ion and hence easier to remove. But this is overwhelmed by a weaker direct ion–ion attraction as well as the "shadowing mechanism" laid out by Lund *et al.*,[36] where the large ion removes additional water from the surface of the small ion. This is included implicitly in the COSMO calculation. As a result there is a strong repulsion of large–small ion pairs at small separations. For two large ions the contact minimum is significantly smaller than for two small ions. This is because the direct electrostatic attraction is substantially weaker for two large ions; although the larger dispersion attraction will somewhat obscure this decrease. However, there is also much less, if any, repulsion at larger separations. This corresponds with the fact that the energy cost of removing water molecules from the surface of large ions is low. The result is that the net interaction is similar to small-small ion pairs. An important corollary of this is that ion–ion interactions cannot be characterized solely by the depth of the potential well at contact.

4.4.2 Non–Electrostatic Ion–Water Contributions. We can see that the cavity and dispersion contributions approximately cancel each other. This is similar to the behaviour of the total solvation energies.[1] However, they do still play an important role in determining the puzzling ion–specific trends. Firstly, the sum of these two contributions is attractive for sodium fluoride and repulsive for cesium fluoride. This can be attributed in part to the significant increase in cation–water dispersion interaction with cation size. Figure 7a presents the

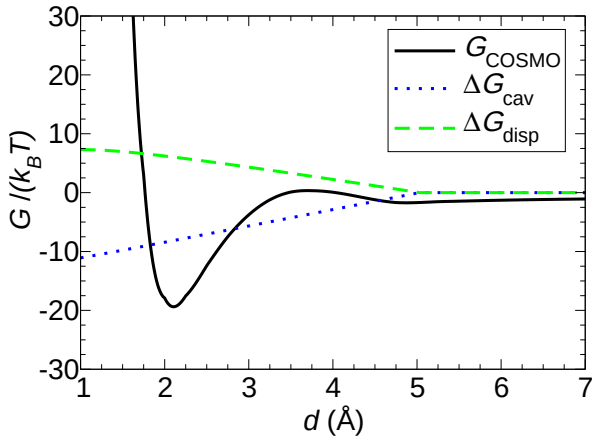

(a) Sodium fluoride

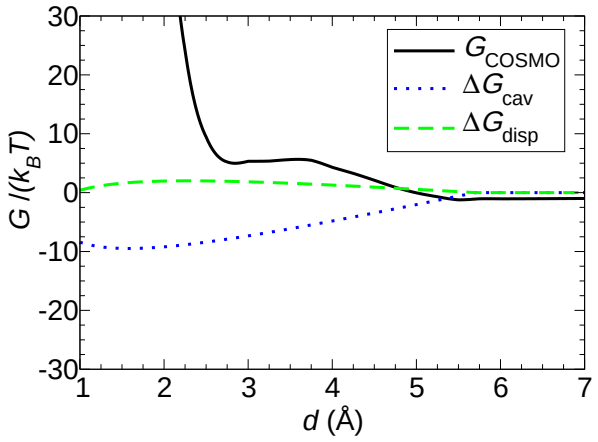

(b) Lithium iodide

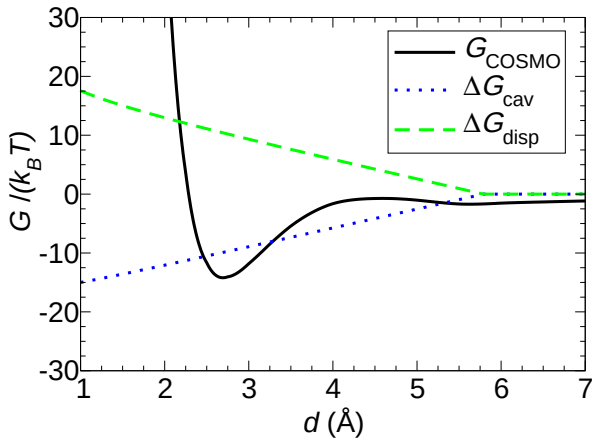

(c) Cesium fluoride

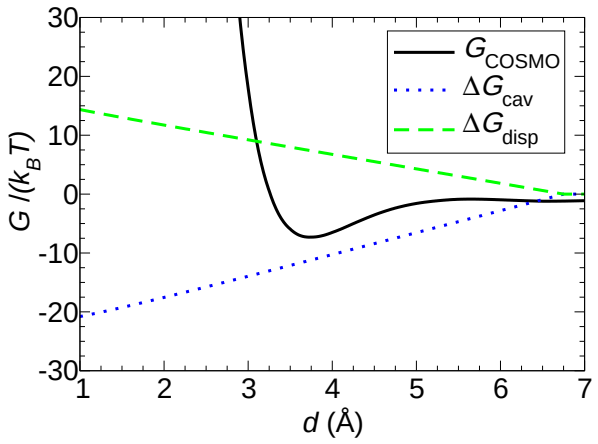

(d) Cesium iodide

Fig. 6 Contributions to the ion–ion interaction potentials, for some representative ion pairs. Calculated using R_{cavA}.

calculation of B coefficients without these contributions. From this figure it is clear that the increase in repulsion with cation size is necessary to reproduce the reversed trend of the fluoride salt series compared with the other anions. This reversed trend can be seen in Figure 4a.

For cesium salts as the anion increases in size the repulsive ion–water dispersion contribution decreases and the cavity attraction increases. This increased attraction with increasing anion size is necessary to reproduce the reversal in the cesium salt trend compared with the other cations. Again, as seen in Figure 7a. For cesium iodide the cavity attraction outweighs the repulsive dispersion contribution. This is important in explaining the fact that large–large ion pairs have a similar affinity to small–small ion pairs. In essence, this corresponds to the hydrophobic type mechanism of large–large ion attraction outlined by Collins.

4.4.3 Ion–Ion Dispersion. Next we probe the importance of the direct ion–ion dispersion interaction by performing the calculation at the Hartree–Fock level, where this contribution is neglected unlike at the MP2 level used previously. It is true that other contributions such as the static polarization interaction may be altered by this change in level of theory. However, the change in the dispersion interaction is likely to dominate, due to the fact that the static electronic effects are damped by the large dielectric response of the water.

This calculation at Hartree–Fock level is presented in Figure 7b. By comparison with Figure 4 it is immediately clear that the Hartree–Fock level gives far inferior results to the MP2 level of theory used above. In addition the observed deviation is exactly what one would expect if the ion–ion dispersion contribution were neglected. Although counter–intuitive we have previously shown that the anionic dispersion interaction is relatively constant with size. On the other hand, the cationic dispersion interaction increases substantially with ion size.[35,37] We see that it is the larger cations that have their B coefficients substantially overestimated. Indeed the difference between Figure 7b and Figure 4b, correlates with Figure 3 of Ref. 35, where DFT–SAPT calculations were performed on ions in vacuum to calculate the strength of their dispersion interaction. This provides strong evidence that the affinity of large ions for each other as constituted in Collins's law is critically dependent on their large direct dispersion interaction.

4.4.4 Polarization Interaction. As the ions approach each other their electric fields will induce a dipole on their partner and result in a net attractive interaction. It is in principle possible to probe the magnitude of this contribution based on the quantum mechanical calculations. However, this extension is beyond the scope of this paper.

5 Conclusion

Future work will require a more satisfactory explanation of the over–attraction, as well as the extension of the approach to multivalent and anisotropic ions, mixed electrolytes, and temperature dependence. This should hopefully validate the theory and begin to allow practical applications in chemical engineering, where these properties are essential. In addition, the model will hopefully be useful in the explanation of more complex traditional Hofmeister series problems, such as those involving ion–protein interactions. For example, the classic Hofmeister effect is the salt dependence of protein precipitation. This effect depends on a balance of ion interactions of two types. One is an ion–surface interaction with the hydrophobic surface of the protein. The second is a pairwise ion–ion interaction with the charged head groups on the protein.[77,78]

In summary, we have generalized our model of ionic solvation energies in order to calculate the free energy of a pair of ions as a function of separation. The calculation includes the essential contributions to these interactions. The cavity sizes were adjusted to match solvation energies, but otherwise there was no deliberate adjustment of ion–specific parameters to achieve agreement. Only two global parameters are necessary to calculate the B coefficients. One is used to normalize the potentials which leads to good direct linear correlation with the experimental B coefficients. A second offset constant is also required. Enthalpy–entropy compensation is hypothesized as the justification for this normalization. This means that the most direct example of Collins's "law of matching water affinity" has been quantitatively reproduced and the driving contributions of this law identified, including the importance of the dispersion interaction.

This work therefore represents, we hope, a significant advance in our understanding of this frustrating and long unsolved problem of physical chemistry. Its resolution serves as a necessary step towards developing a quantitative and predictive understanding of the interaction of solutes in water.

6 Appendix

In order to perform the integrals in Eqs. 9–11 we used toroidal coordinates as given in Ref. 79:

$$x = \frac{R_0\sqrt{1-\xi^2}\cos(\phi)}{1-\xi\cos(\eta)} \tag{21}$$

$$y = \frac{R_0\sqrt{1-\xi^2}\sin(\phi)}{1-\xi\cos(\eta)} \tag{22}$$

$$z = \frac{R_0\xi\sin(\eta)}{1-\xi\cos(\eta)} \tag{23}$$

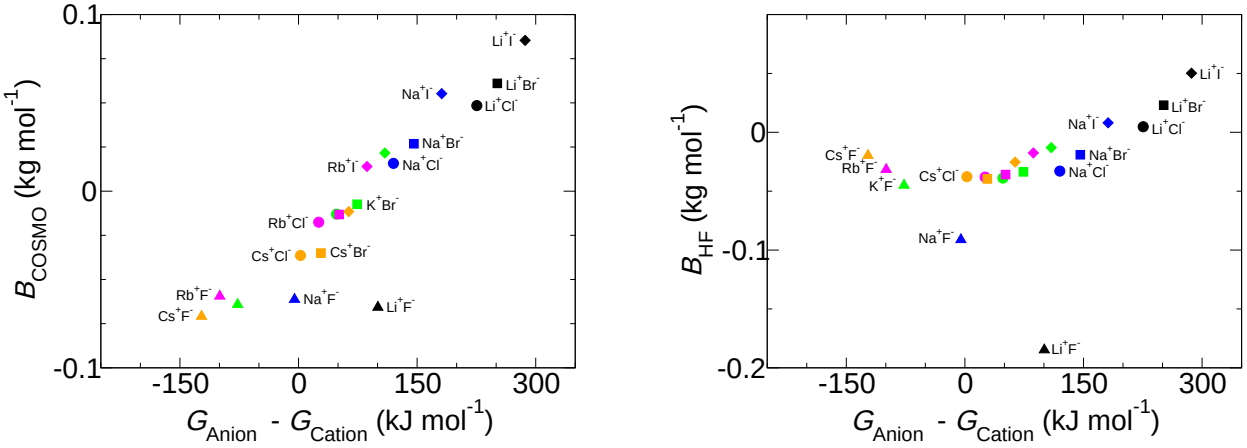

(a) COSMO only **(b)** Hartree–Fock

Fig. 7 The theoretical B coefficients vs. the difference in the solvation energy of the ions. (a) Only the COSMO contribution is used, i.e, with $\Delta G_{\text{cav}} = \Delta G_{\text{disp}} = 0$. (b) The Hartree–Fock level of theory is used instead of MP2 for the COSMO contribution. R_{cavA} is used in both cases.

Where $0 < \eta < 2\pi, 0 < \phi < 2\pi, 0 < \xi < 1$

Surfaces of constant η give spherical bowls with a centre on the z axis. They are cut off in the xy plane with at a circle of radius R_0. If $\eta_c < \pi$ the sphere is above the xy plane((+)ve z) and taking the surface with $\eta_n = \eta_c + \pi$ gives the rest of the circle below the xy plane. We can easily create the surface of two overlapping spherical cavities in this coordinates system. Given the radii of the two cavities ($R_{\text{cav},i}$ and $R_{\text{cav},j}$) and the separation (d) between their centres, we can give the z coordinates of the centre of the two spheres:

$$c_i = \frac{d^2 - R_{\text{cav},j}^2 + R_{\text{cav},i}^2}{2d} \tag{24}$$

$$c_j = \frac{-d^2 + R_{\text{cav},i}^2 - R_{\text{cav},j}^2}{2d} \tag{25}$$

The values of constant η which give the surfaces are:

$$\eta_i = \arccos\left(\frac{c_i}{R_{\text{cav},i}}\right) \tag{26}$$

$$\eta_j = \arccos\left(\frac{c_j}{R_{\text{cav},j}}\right) + \pi \tag{27}$$

Also $R_0 = R_{\text{cav},i}\sin(\eta_i) = R_{\text{cav},j}\sin(\eta_j)$. The positions of the centres can be written in toroidal coordinates as $\xi_{c,i} = \xi_{c,j} = 1, \phi_{c,i} = \phi_{c,j} = 0$, and $\eta_{c,i} = 2\arctan(\frac{R_0}{c_i})$ and $\eta_{c,j} = 2\arctan(\frac{R_0}{c_j}) + 2\pi$ For ion i we can then rewrite the two integrals in each of Eqs. 9–11 as

$$\frac{\left[\int_0^{\eta_i} + \int_{\eta_j}^{2\pi}\right]\int_0^1\int_0^{2\pi} d\phi d\xi d\eta (J_t) U(\xi,\eta)}{4\pi\int_{R_{\text{cav},i}}^{\infty} dr r^2 U(r)} \tag{28}$$

Where $U(r) = 1/r^{2n}$. From the transformation equations above we also have:

$$U(\xi,\eta) = 1/(x(\xi,\eta) + y(\xi,\eta)^2 + (z(\xi,\eta) - z(\xi_{c,i},\eta_{c,i}))^2)^n \tag{29}$$

n is 3 for dipolar, 4 for quadrupole and 6 for octupole. The Jacobian is

$$(J_t) = \frac{R_0^3 \xi}{(1 - \xi\cos(\eta))^3} \tag{30}$$

This integral can be solved analytically, and for the dipole operator we arrive at:

$$\frac{\pi}{6R_0^3}(\cos(\eta - \eta_{c,i}) - 2)\cot\left(\frac{\eta - \eta_{c,i}}{2}\right)\csc\left(\frac{\eta - \eta_{c,i}}{2}\right)^2 \times\sin\left(\frac{\eta_{c,i}}{2}\right)^6\Bigg]_{\eta=\eta_j}^{\eta=\eta_i} \tag{31}$$

with similar although significantly longer expressions for the quadrupole and octupole moments. This is straightforwardly generalized for the second ion by replacing $z(\xi_{c,i},\eta_{c,i})$ with $z(\xi_{c,j},\eta_{c,j})$ in Eq. 29 and $R_{\text{cav},i}$ with $R_{\text{cav},j}$ in the denominator of Eq. 28.

7 Acknowledgements

This work was supported by the NCI National Facility at the ANU.

References

1 T. T. Duignan, D. F. Parsons and B. W. Ninham, *J. Phys. Chem. B*, 2013, **117**, 9421–9429.
2 T. T. Duignan, D. F. Parsons and B. W. Ninham, *J. Phys. Chem. B*, 2014, **118**, 8700–8710.
3 B. W. Ninham and P. Lo Nostro, *Molecular Forces and Self Assembly*, Cambridge University Press, Cambridge, 2010.
4 P. Lo Nostro and B. W. Ninham, *Chem. Rev.*, 2012, **112**, 2286–2322.
5 P. Debye and E. Hückel, *Phys. Z.*, 1923, **24**, 185–206.
6 R. A. Robinson and R. H. Stokes, *Electrolyte Solutions*, Butterworth & Co., Devon, 1959.
7 K. S. Pitzer, *J. Phys. Chem.*, 1972, **77**, 268–277.
8 L. A. Bromley, *AIChE J.*, 1973, **19**, 313–320.
9 B. A. Pailthorpe, D. J. Mitchell and B. W. Ninham, *J. Chem. Soc., Faraday Trans. 2*, 1984, **80**, 115–139.
10 M. A. Knackstedt and B. W. Ninham, *J. Phys. Chem.*, 1996, **100**, 1330–1335.
11 P. S. Ramanathan and H. L. Friedman, *J. Chem. Phys.*, 1971, **54**, 1086–1099.
12 C.-C. Chen, H. I. Britt, J. F. Boston and L. B. Evans, *AlChe*, 1982, **28**, 588–596.
13 C.-C. Chen and Y. Song, *AIChE J.*, 2004, **50**, 1928–1941.
14 Y. Song and C.-C. Chen, *Ind. Eng. Chem. Res.*, 2009, **48**, 7788–7797.
15 J.-F. Lu, Y.-X. Yu and Y.-G. Li, *Fluid Phase Equilib.*, 1993, **85**, 81–100.
16 J.-P. Simonin, O. Bernard and L. Blum, *J. Phys. Chem. B*, 1998, **102**, 4411–4417.
17 Y. V. Kalyuzhnyi, V. Vlachy and K. A. Dill, *Phys. Chem. Chem. Phys.*, 2010, 6260–6266.
18 C.-L. Lin, L.-S. Lee and H.-C. Tseng, *Fluid Phase Equilib.*, 1993, **90**, 57–79.
19 X. Ge, X. Wang, M. Zhang and S. Seetharaman, *J. Chem. Eng. Data*, 2007, **52**, 538–547.
20 S. Wang, Y. Song and C.-C. Chen, *Ind. Eng. Chem. Res.*, 2011, **50**, 176–187.
21 P. J. Lenart, A. Jusufi and A. Z. Panagiotopoulos, *J. Chem. Phys.*, 2007, **126**, 044509.
22 I. Kalcher and J. Dzubiella, *J. Chem. Phys.*, 2009, **130**, 134507.
23 L. Vrbka, M. Lund, I. Kalcher, J. Dzubiella, R. R. Netz and W. Kunz, *J. Chem. Phys.*, 2009, **131**, 154109.
24 J. J. Molina, J.-F. Dufrêche, M. Salanne, O. Bernard and P. Turq, *J. Chem. Phys.*, 2011, **135**, 234509.
25 L. Petit, R. Vuilleumier, P. Maldivi and C. Adamo, *J. Chem. Theory Comput.*, 2008, **4**, 1040–1048.
26 M. Vazdar, F. Uhlig and P. Jungwirth, *J. Phys. Chem. Lett.*, 2012, **3**, 2021–2024.
27 E. Pluhařová, O. Marsalek, B. Schmidt and P. Jungwirth, *J. Phys. Chem. Lett.*, 2013, **4**, 4177–4181.
28 Y. Luo, W. Jiang, H. Yu, A. D. MacKerell and B. Roux, *Faraday Discuss.*, 2013, **160**, 135–149.
29 W. Kunz, *Specific Ion Effects*, World Scientific, 2010.
30 C. J. Fennell, A. Bizjak, V. Vlachy and K. A. Dill, *J. Phys. Chem. B*, 2009, **113**, 6782–6291.
31 M. Fyta, I. Kalcher, J. Dzubiella, L. Vrbka and R. R. Netz, *J. Chem. Phys.*, 2010, **132**, 024911.
32 M. Fyta and R. R. Netz, *J. Chem. Phys.*, 2012, **136**, 124103.
33 K. D. Collins, *Biophys. J.*, 1997, **72**, 65–76.
34 W. Kunz, *Curr. Opin. Colloid Interface Sci.*, 2010, **15**, 34–39.
35 T. T. Duignan, D. F. Parsons and B. W. Ninham, *Chem. Phys. Lett.*, 2014, **608**, 55–59.
36 M. Lund, B. Jagoda-Cwiklik, C. E. Woodward, R. Vácha and P. Jungwirth, *J. Phys. Chem. Lett.*, 2010, **1**, 300–303.
37 T. T. Duignan, D. F. Parsons and B. W. Ninham, *J. Phys. Chem. B*, 2013, **117**, 9412–9420.
38 T. T. Duignan, D. F. Parsons and B. W. Ninham, *J. Phys. Chem. B*, 2014, **118**, 3122–3132.
39 W. Kunz, L. Belloni, O. Bernard and B. W. Ninham, *J. Phys. Chem. B*, 2004, **108**, 2398–2404.
40 A. A. Rashin, *J. Phys. Chem.*, 1989, **93**, 4664–4669.
41 B. W. Ninham and R. A. Sammut, *J. Theor. Biol.*, 1976, **56**, 125–149.
42 A. Klamt and G. Schüürmann, *J. Chem. Soc. Perkin Trans. 2*, 1993, 799–805.
43 A. Klamt, *Wiley Interdiscip. Rev.: Comput. Mol. Sci.*, 2011, **1**, 699–709.
44 L. R. Pratt, G. J. Tawa, G. Hummer, A. E. García and S. A. Corcelli, *Int. J. Quantum Chem.*, 1997, **64**, 121–141.
45 Y. Levin, A. P. dos Santos and A. Diehl, *Phys. Rev. Lett.*, 2009, **103**, 257802.
46 D. Chandler, *Nature*, 2005, **437**, 640–647.
47 S. J. Wodak and J. Janin, *Proc. Natl. Acad. Sci. U. S. A.*, 1980, **77**, 1736–1740.
48 A. G. Donchev, *J. Chem. Phys.*, 2006, **125**, 074713.
49 A. Ben-Naim, *Hydrophobic Interactions*, Plenum Press, New York and London, 1980, p. 311.
50 W. G. Mcmillan and J. E. Mayer, *J. Chem. Phys.*, 1945, **13**, 276–305.
51 C. Bretti, C. Foti, N. Porcino and S. Sammartano, *J. Solution Chem.*, 2006, **35**, 1401–1415.
52 E. A. Guggenheim, *Applications of Statistical Mechanics*, Clarendon Press, Oxford, 1966, p. 211.
53 H. L. Friedman, *J. Solution Chem.*, 1972, **1**, 413–417.
54 *Turbomole V6.4 2012. A development of University of Karlsruhe and Forschungszentrum Karlsruhe GmbH; available from http://www.turbomole.com.*
55 R. Ahlrichs, M. Bär, M. Häser, H. Horn and C. Kölmel, *Chem. Phys. Lett.*, 1989, **162**, 165–169.
56 F. Weigend, F. Furche and R. Ahlrichs, *J. Chem. Phys.*, 2003, **119**, 12753.
57 F. Weigend and R. Ahlrichs, *Phys. Chem. Chem. Phys.*, 2005, **7**, 3297–3305.
58 C. Hättig, *Phys. Chem. Chem. Phys.*, 2005, **7**, 59–66.
59 A. Hellweg, C. Hättig, S. Höfener and W. Klopper, *Theor. Chem. Acc.*, 2007, **117**, 587–597.
60 T. Leininger, A. Nicklass, W. Küchle, H. Stoll, M. Dolg and A. Bergner, *Chem. Phys. Lett.*, 1996, **255**, 274–280.
61 K. A. Peterson, D. Figgen, E. Goll, H. Stoll and M. Dolg, *J. Chem. Phys.*, 2003, **119**, 11113–11123.
62 J. Liu, C. P. Kelly, A. C. Goren, A. V. Marenich, C. J. Cramer, D. G. Truhlar and C.-G. Zhan, *J. Chem. Theory Comput.*, 2010, **6**, 1109–1117.
63 M. Häser and R. Ahlrichs, *J. Comput. Chem.*, 1989, **10**, 104–111.
64 F. Weigend and M. Häser, *Theor. Chem. Acc.*, 1997, **97**, 331–340.
65 F. Weigend, M. Häser, H. Patzelt and R. Ahlrichs, *Chem. Phys. Lett.*, 1998, **294**, 143–152.
66 J. G. Ángyán, *Chem. Phys. Lett.*, 1995, **241**, 51–56.
67 I. C. Gerber and J. G. Ángyán, *J. Chem. Phys.*, 2007, **126**, 044103.
68 E. Sobolewski, M. Makowski, C. Czaplewski, A. Liwo, S. Oldziej and H. A. Scheraga, *J. Phys. Chem. B*, 2007, **111**, 10765–10774.
69 M. Lukšič, C. J. Fennell and K. A. Dill, *J. Phys. Chem. B*, 2014, **118**, 8017–8025.
70 R. Geney, M. Layten, R. Gomperts, V. Hornak and C. Simmerling, *J. Chem. Theory Comput.*, 2006, **2**, 115–127.
71 E. Gallicchio, K. Paris and R. M. Levy, *J. Chem. Theory Comput.*, 2009, **5**, 2544–2564.
72 E. Pluhařová, P. E. Mason and P. Jungwirth, *J. Phys. Chem. A*, 2013, **117**, 11766–11773.
73 L. R. Pratt, G. Hummer and A. E. García, *Biophys. Chem.*, 1994, **51**, 147–165.

74 S. Marčelja and N. Radić, *Chem. Phys. Lett.*, 1976, **42**, 129–130.
75 Z. Yu, M. P. Jacobson, J. Josovitz, C. S. Rapp and R. A. Friesner, *J. Phys. Chem. B*, 2004, **108**, 6643–6654.
76 A. J. Ballard and C. Dellago, *J. Phys. Chem. B*, 2012, **116**, 13490–13497.
77 L. Medda, C. Carucci, D. F. Parsons, B. W. Ninham, M. Monduzzi and A. Salis, *Langmuir*, 2013, **29**, 15350–15358.
78 M. Lund, L. Vrbka and P. Jungwirth, *J. Am. Chem. Soc.*, 2008, **130**, 11582–11583.
79 J. W. Bates, *J. Math. Phys.*, 1997, **38**, 3679–3691.